generally leads to the generation of a broad molecular weight distribution with one or more "shoulders". See also: a) R. Leino, H. J. G. Luttikhedde, P. Lehmus, C.-E. Wilén, R. Sjöholm, A. Lehtonen, J. V. Seppälä, J. H. Näsman, *J. Organomet. Chem*. **1998**, *559*, 65 – 72; b) D. W. Stephan, J. C. Stewart, F. Guérin, R. E. v. H. Spence, W. Xu, D. G. Harrison, *Organometallics* **1998**, *18*, 1116 – 1118; c) G. H. Llinas, R. O. Day, M. D. Rausch, J. C. W. Chien, *Organometallics* **1993**, *12*, 1283 – 1288, and references therein; d) A. Yano, S. Hasegawa, T. Kaneko, M. Sone, M. Sato, *Macromol. Chem. Phys.* **1999**, *200*, 1542 – 1553; C. Janiak, K. C. H. Lange, U. Versteeg, D. Lentz, P. H. M. Budzelaar, *Chem. Ber*. **1996**, *129*, 1517 – 1529.

[4] P. Jutzi, T. Redeker, *Eur. J. Inorg. Chem*. **1998**, 663 – 674.

[5] C. Müller, D. Lilge, M. O. Kristen, P. Jutzi (Elenac GmbH), patent application OZ 0775/00013 (February 1, 1999).

[6] a) J. E. Park, B.-J. Bae, Y. Kim, J. T. Park, I.-H. Suh, *Organometallics* **1999**, *18*, 1059 – 1067; b) Y. Kim, J. H. Kim, J. E. Park, H. Song, J. T. Park, *J. Organomet. Chem*. **1997**, *545*/*546*, 99 – 103.

[7] The intramolecularly donor-stabilized complex $[\{\eta^5\text{-}C_5H_3(CH_2CH_2NMe_2)CMe_2\text{-}\eta^5\text{-}C_{13}H_8\}ZrCH_3]^+B(C_6F_5)_4^-$ was isolated and is not active in the polymerization catalysis. However, after addition of AlR_3, a catalytically active species was obtained.

[8] a) P. Jutzi, T. Redeker, B. Neumann, H.-G. Stammler, *Organometallics* **1996**, *15*, 4153 – 4161; b) P. Jutzi, T. Redeker, B. Neumann, H.-G. Stammler, *Chem. Ber*. **1996**, *129*, 1509 – 1515.

[9] Polymerization of ethylene with **4**/MAO: see Experimental Section; Zr:Al = 1:1000, $n(Zr) = 3 \times 10^{-5}$ mol. Polymerization temperature: $T = 50\,^{\circ}C$, activity: 59 kg_{PE} $(mol_{Zr}\,h\,bar)^{-1}$.

[10] R. H. Boyd, P. J. Phillips in *The Science of Polymer Molecules*, Cambridge University Press, **1993**, 18 – 59.

[11] Synthesis of **1**: P. Jutzi, C. Müller, *Synthesis*, in press.

Real Space Observation of a Chiral Phase Transition in a Two-Dimensional Organic Layer**

Matthias Böhringer,* Wolf-Dieter Schneider, and Richard Berndt

Chiral discrimination between mirror-image stereoisomers can lead to the spontaneous separation of a racemic mixture into enantiomerically pure phases.[1] In three-dimensional systems the formation of these conglomerates is the exception rather than the rule; most racemic mixtures crystallize as racemates with the unit cell composed of an equal number of molecules with opposite chirality or as random solid solutions. It was originally proposed by Stewart and Arnett that confinement to two dimensions (2D) enhances chiral discrimination between enantiomers.[2] Most racemic 2D systems investigated experimentally so far, with respect to spontaneous breaking of the mirror symmetry, are Langmuir films of amphiphilic molecules with one or more asymmetric carbon atoms.[2–7] Atomic force microscopy (AFM) observations by Eckhardt et al. of enantiomorphic supramolecular structures evolving from a racemic mixture of a chiral amphiphile have been interpreted in terms of chiral segregation.[4] However, chiral packing of achiral molecules has also been observed to cause enantiomorphous structures.[8–12] Therefore, the observation of chiral supramolecular structures alone does not prove chiral phase separation.

A straightforward proof for chiral segregation is the direct determination of the chirality of individual molecules. Scanning-tunneling microscopy (STM) has been successfully applied to determine the conformation and chirality of individual molecules.[13, 14] Lopinski et al. used STM to determine the absolute configuration of isolated chiral centers.[14] The same technique was employed by de Feyter et al. to identify the positions of asymmetric carbon atoms within homochiral domains of a chiral terephthalic acid derivative.[15] In the present paper, we report the first real space observation of a coverage-driven chiral phase transition from a conglomerate to a racemate at low and high molecular coverages, respectively. The chirality of individual molecules is determined from high resolution STM images which closely reflect the asymmetric electronic structure of the molecules. From the STM data, models are deduced for the distinct chiral and achiral phases, revealing the driving force for chiral symmetry breaking.

The substrate used is reconstructed Au(111) which is comprised of uniaxial domains of alternating face centred cubic (fcc) and hexagonal close packed (hcp) stacking of the surface atoms (Figure 1 a). The domain walls form a herringbone pattern visible as bright stripes in the STM topographs.

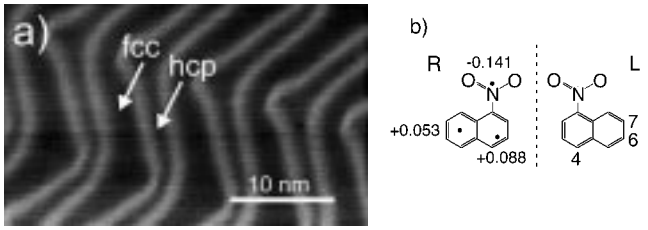

Figure 1. a) STM topograph of the reconstructed Au(111) surface. Broad and narrow dark stripes correspond to domains with surface atoms in fcc or hcp positions, respectively. The transition regions (domain walls) separating fcc and hcp regions appear as bright stripes. b) 1-Nitronaphthalene (NN) in a planar adsorption geometry on Au(111) is 2D chiral. Molecules with the nitro group attached to the left/right carbon ring are denoted as L/R-enantiomers. The nitro group has a net negative charge; the two carbon rings are positively charged.[17] The centres of mass of the respective charges are marked with dots.

1-Nitronaphthalene (NN, Figure 1 b) adsorbs with the naphthalene system parallel to the Au(111) surface.[16] This geometry imposes a chirality onto the NN molecules which is not present in the gas phase. An adsorbed molecule and its mirror image can not be superimposed by rotation and translation within the surface plane (Figure 1 b). On the

[*] Dr. M. Böhringer,[+] Prof. Dr. W.-D. Schneider
Institut de Physique de la Matière Condensée
Université de Lausanne
1015 Lausanne (Switzerland)
E-mail: Matthias.Boehringer@de.bosch.com
Prof. Dr. R. Berndt
Christian-Albrechts-Universität Kiel
Institute for Experimental and Applied Physics
[+] New address:
Robert Bosch GmbH, RtW1/FIW4
Postfach 1342, 72703 Reutlingen (Germany)
Fax: (+49) 7121-35-1593

[**] We are delighted to thank K. Morgenstern, F. Mauri, A. de Vita, and R. Car for helpful discussions.

  0570-0833/00/3904-0792 $ 17.50+.50/0

Au(111) surface equal amounts of left- and right-handed (L and R, respectively) NN molecules are present; these form a racemic mixture.

Below a temperature of 100 K the NN molecules aggregate into distinct structures whose dimensionality depends on the coverage. At 50 K and coverages below 0.25 monolayers (ML), monodisperse zero-dimensional molecular clusters are observed.[17, 18] In a medium coverage range, one-dimensional (1D) structures prevail. These are straight molecular double chains within the fcc domains (Figure 2a, 0.3 ML) and, at higher coverages, also within the hcp domains (Figure 2b, 0.4 ML). Moreover, zig-zag patterns are observed within fcc domains at 0.4 ML coverage. Finally, at full monolayer coverage 1D and 2D periodic molecular structures coexist on the surface (Figures 2c, d).

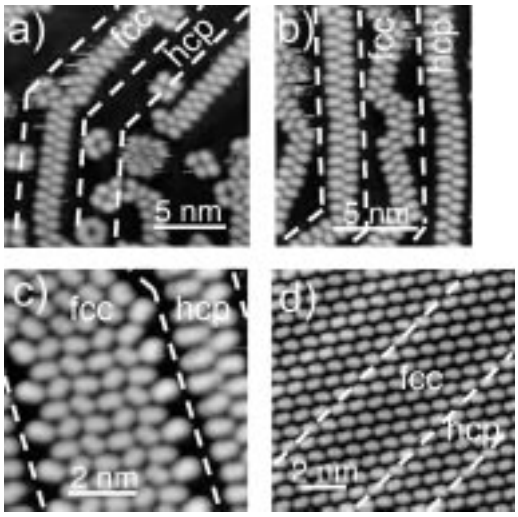

Figure 2. Molecules are imaged as bright ellipsoids (long axis $\approx$ 1 nm). a) STM image recorded at 0.3 ML coverage of NN. Straight molecular double chains follow the fcc domains, while a few small aggregates are observed within the hcp domains. Domain walls separating fcc and hcp domains are indicated by broken lines. b) STM image recorded at 0.4 ML coverage of NN. The linear structure is observed within hcp domains as well. In fcc domains, chains now form a zig-zag pattern while the domain walls are largely free of molecules. c) and d) STM image recorded at monolayer coverage. 1D structures within fcc and hcp domains (c) coexist with a 2D periodic phase (d).

Although the electronic structure of NN is strongly asymmetric owing to the nitro group, the molecule is imaged as a rather symmetrical ellipsoid over a wide range of tunneling parameters and the enantiomers cannot be distinguished (Figure 2 and Figure 3a). However, when occupied sample states are probed at a tunneling voltage of $V = -2.3$ V, intramolecular structure is resolved which reflects the asymmetry of the molecule and enables enantiomeric discrimination. In Figure 3b each molecule appears as three bright maxima and a fourth very weak maximum. Two of the bright maxima are located at the periphery of the double chain while the third bright and the weak maxima point inwards. This intramolecular contrast pattern shows the expected handedness.

The charge density calculated for the highest occupied molecular orbital (HOMO) of the NN molecule 5 Å above

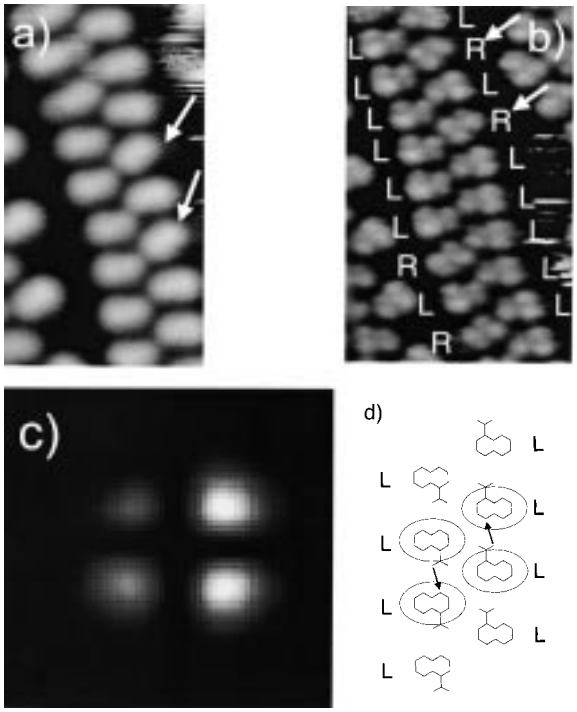

Figure 3. a) Segment of an NN double chain as typically imaged at low tunneling voltages (-1.2 V). b) At high negative tunneling voltage (-2.3 V) each molecule appears as three bright maxima and one very weak maximum. This intramolecular contrast pattern reflects the asymmetry of the NN molecules and allows for the discrimination between the NN enantiomers. Defect free, straight sections of the double chains are composed of exclusively one enantiomer. Molecules with opposite chirality (marked by arrows) are rotated. c) Charge density of the NN HOMO, calculated 5 Å above the molecular plane for an L type molecule (from Ref. [17]). The weakest maximum corresponds to the part of the naphthalene system where the nitro group is attached. The chirality is attributed to the molecules by comparison with this calculated charge density. d) Model of the enantiopure double chain structure (from Ref. [17]). Arrows denote the hydrogen bonds. The ellipsoids indicate the shape of the molecules observed in low-resolution images.

the molecular plane (Figure 3c) closely resembles the observed submolecular structure.[17] The weakest maximum is associated with the part of the naphthalene system which carries the substituent. This pattern may be understood in terms of the strong charge-pulling effect of the nitro group on the NN π-electron system. From this agreement we conclude that, at a bias voltage of -2.3 V, the submolecular image contrast is dominated by an NN HOMO-derived sample state. At lower bias voltage, hybridization with substrate states results in the nearly symmetrical appearance of the molecules.[19] The high-resolution data in Figure 3b enables a direct determination of the handedness of each molecule and leads to the model reproduced in Figure 3d. This model has been confirmed by molecular dynamics simulations on the basis of long range electrostatic interactions and short range van der Waals interactions between the NN molecules.[17] Within each single strand the molecules are arranged in a "head to tail" configuration with hydrogen bonds between a negatively charged oxygen atom and the "back" hydrogen atom on the carbon atom C4 of a neighbouring NN molecule. The second strand is rotated by 180° and shifted by half a period such that opposite charges are close to each other. From the high-

  0570-0833/00/3904-0793 $ 17.50+.50/0

resolution images and the theoretical modeling we conclude that straight, defect-free segments of the double chains consist of exclusively one NN enantiomer (L type in Figure 3b), thus representing a 1D conglomerate.

Sporadically, molecules in the L conglomerate are exchanged with a R enantiomer (arrows in Figure 3b). These molecules are rotated by $\approx 25^\circ$ (arrows in Figure 3a). This specific rotation allows for hydrogen bonding to the back hydrogen atom of the adjacent molecule (Figure 4a). At low coverages we find less than 2% of these defects in double chains, corresponding to an enantiomeric excess $> 96\%$.

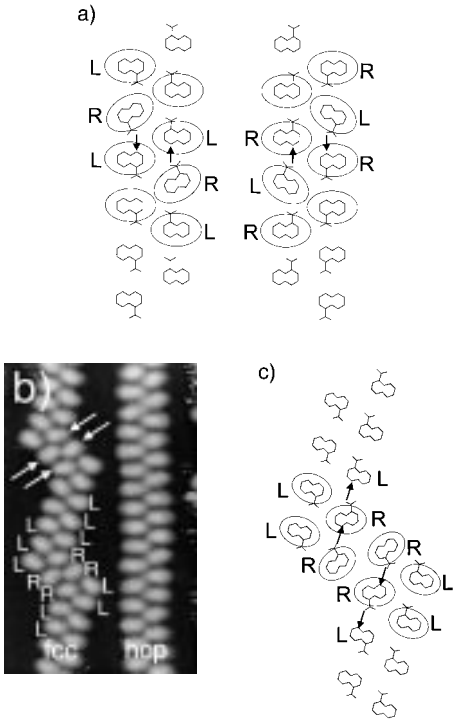

Figure 4. a) Model of an L type double chain with some isolated molecules of opposite chirality incorporated into the otherwise enantiopure structure. b) Typical geometry of the zig-zag structure observed within fcc domains at 0.4 ML coverage. The zig-zag geometry in the upper and lower half of the image is identical. Arrows mark rotated molecules which terminate straight segments. c) Model of the zig-zag structure. Minimal segments of chains with opposite chirality are incorporated into the otherwise enantiopure double chains. The attribution of L and R to the molecules in (b) corresponds to this model.

Moreover, one observes that molecules with opposite chirality can introduce kinks into the otherwise straight molecular chains. The zig-zag arrangement within the fcc domains shown in Figure 2b indicates that with increasing coverage more and more molecules with opposite handedness are built into the double chains, corresponding to a gradual transition from a conglomerate to a racemate. In the typical zig-zag geometry, straight segments terminate with two rotated molecules (arrows in Figure 4b). This structure can be modeled by introducing minimal segments of opposite chirality into the otherwise enantiopure double chains (Figure 4c).

Packing even more NN molecules onto fcc sites results in the structure shown in Figure 2c. Rows composed of five molecules are stacked along the fcc domains and in this low resolution image adjacent rows appear enantiomorphous. Indeed, the corresponding high resolution image (Figure 5a) reveals that neighboring rows are composed of opposite enantiomers. The surface unit cell is therefore comprised of an

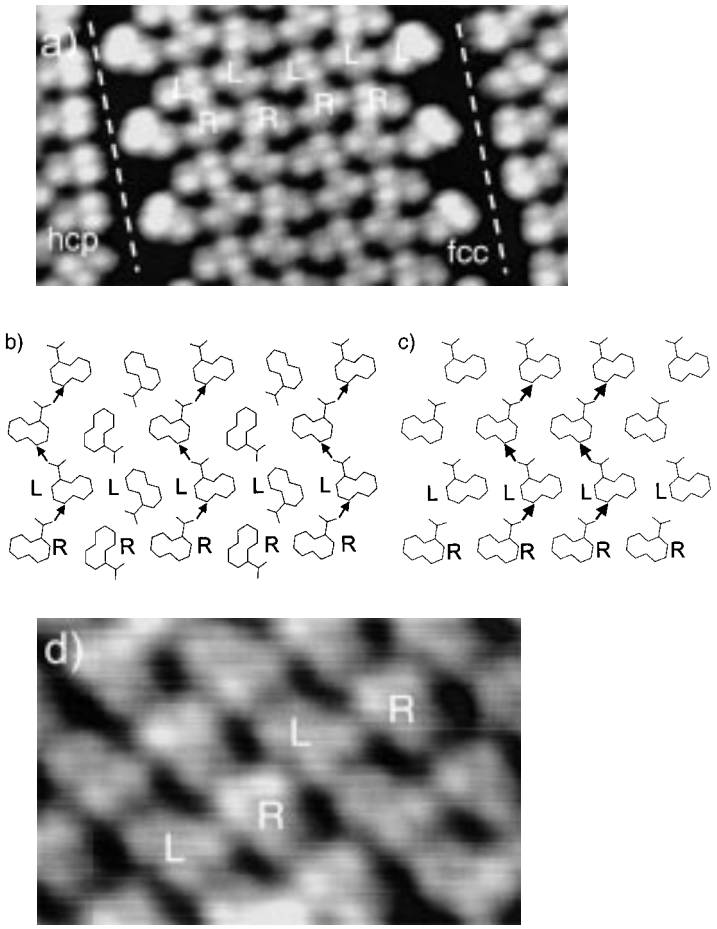

Figure 5. a) High-resolution image of the densely packed structure in the fcc domains of Figure 2c. Along the fcc domain, molecules in adjacent rows show opposite chirality. The structure therefore represents a quasi-1D racemate. In the hcp domains enantiopure molecular double chains persist but with an increased density of chiral defects. b) Model of the structure in the fcc domains. Half of the molecules form hydrogen bonds (arrows) similar to the "head to tail" geometry described for the double chain structure. However, contrary to the enantiopure double chains the hydrogen bonds now occur between molecules of opposite chirality. c) Rotation of half of the molecules in (b) by $\pm 120^\circ$ results in a racemate structure where all molecules take part in hydrogen bonding. d) High resolution images of the 2D structure shown in Figure 2d are consistent with the model reproduced in (c).

equal number of both enantiomers so that the structure is a 1D racemate. Half of the molecules form hydrogen bonds similar to the "head to tail" geometry described above (arrows in the model Figure 5b). Here, however, hydrogen bonds occur between molecules of different chirality. For the other molecules, the negative oxygen atoms point towards (positive) hydrogen atoms on the carbon atoms C6 and C7 of adjacent NN molecules. Rotation of these molecules by approximately $\pm 120^\circ$ results in the racemate structure depicted in Figure 5c where all molecules form "head to tail" hydrogen bonds to neighbouring molecules of opposite

  0570-0833/00/3904-0794 $ 17.50+.50/0

chirality. This structure is consistent with the high-resolution image (Figure 5d) of the 2D periodic molecular arrangement shown in Figure 2d. At monolayer coverage it coexists with the 1D racemate in fcc domains and the 1D conglomerate in hcp domains (Figure 2c). The average density of molecules in the 1D and 2D structures (Figure 2c, d) are identical. In Figure 2c the lower density of molecules in the double rows and the depletion of the domain walls from molecules is compensated for by a more dense packing in the fcc domains.

The structural transformations described above represent a transition from a conglomerate at low coverages into a racemate at high coverage. They may be interpreted in terms of two driving forces. First, electrostatics favor interactions among identical enantiomers. Second, adsorption is strongest on fcc sites of the reconstructed Au(111) surface, weaker on hcp sites, and weakest on the transition regions between fcc and hcp domains (domain walls). As a consequence of these trends, at low molecular densities NN assembles into straight enantiopure chains which are located in fcc domains (Figure 2a). At higher coverages, the length of the double chains in the fcc domains increases through the formation of a zig-zag structure. This, however, costs electrostatic energy since opposite enantiomers have to be incorporated into the otherwise homochiral chains. Likewise, electrostatically optimal, straight, enantiopure chains are formed at energetically less favorable hcp sites. No kinks are introduced into the chains within hcp domains because any zig-zag would expel molecules from these narrow domains into unfavorable sites on top of the domain walls. At monolayer coverage, a 2D periodic racemic structure with dominating heterochiral interactions is formed, which does not follow the surface reconstruction (Figure 2d). This phase is instable and can decay into a 1D racemate within fcc domains and a 1D conglomerate within hcp domains (Figure 2c).

Our observations show similarities with a scenario described by Andelman and de Gennes.[20] For amphiphiles in an adsorption geometry where three of the four distinct substituents of an asymmetric carbon atom are confined to two dimensions, spontaneous chiral segregation was predicted, provided that there are strong electrostatic interactions between two oppositely charged groups and a third neutral in-plane substituent which interacts equally with the two charged groups. The predicted ground state structure is an enantiopure 2D hexagonal lattice. In the case of NN, at low coverages, the enantiopure double chain structure is likewise determined by the strong interaction between the opposite charges localized at the oxygen atoms and the hydrogen atom on the carbon atom C4. However, unlike the tripodal molecules discussed in Ref. [20], an additional net positive charge is localized at the second carbon ring of the naphthalene system (Figure 1b) which prevents the formation of the predicted homochiral 2D structure. Rather, as long as the density of molecules is low, a linear 1D structure occurs where the positive charge of the second carbon ring is expelled to the periphery. At high NN coverage, the strong competition in the electrostatic interactions between all three groups is expected to result in frustration effects.[20] The interaction with the reconstructed Au(111) substrate may then become important in destabilizing the 2D periodic, heterochiral, monolayer structure with respect to a mixture of a 1D heterochiral and a 1D homochiral phase.

In summary, we have observed in real space a coverage-driven transition from a conglomerate to a racemate for the 2D chiral molecule 1-nitronaphthalene on Au(111). High resolution STM images directly reveal the chirality of the adsorbed molecules and lead to models for the chiral and achiral phases. The observed spontaneous breaking of the chiral symmetry at low coverages has been discussed within an electrostatic model for the intermolecular interactions.

Experimental Section

The experiments were performed under ultra high vacuum (base pressure $< 1 \times 10^{-10}$ mbar) with a custom-built low-temperature scanning tunneling microsope.[21] Clean Au(111) surfaces were obtained by repeated sputter–anneal cycles. Purified NN was admitted to the vacuum chamber by a leak valve from a gas handling line ($\approx$350 K) onto the sample at 295 K. The amount of NN dosed onto the surface was controlled by the increase of the total pressure inside the vacuum chamber ($2-5 \times 10^{-8}$ mbar) and the time of exposure (4–20 s). Subsequently, the sample was cooled to 50 K and constant-current STM images were recorded. For experiments at distinct coverages the sample was warmed up, cleaned, redosed and cooled to 50 K as before.

Received: May 31, 1999
Revised: August 9, 1999 [Z13489]

[1] L. Pasteur, *C. R. Hebd. Seances Acad. Sci.* **1848**, *26*, 535–539.
[2] M. V. Stewart, E. M. Arnett in *Topics in Stereochemistry* (Eds.: N. L. Allinger, E. L. Eliel, S. H. Wilen), Wiley, New York, **1982**, pp. 195–262.
[3] R. M. Weis, H. M. McConnell, *Nature* **1984**, *310*, 47–49.
[4] C. J. Eckhardt, N. M. Peachey, D. R. Swanson, J. M. Takacs, M. A. Khan, X. Gong, J. H. Kim, J. Wang, R. A. Uphaus, *Nature* **1993**, *362*, 614–616.
[5] P. Nassoy, M. Goldmann, O. Bouloussa, F. Rondelez, *Phys. Rev. Lett.* **1995**, *75*, 457–460.
[6] F. Stevens, D. J. Dyer, D. M. Walba, *Angew. Chem.* **1996**, *108*, 955–957; *Angew. Chem. Int. Ed. Engl.* **1996**, *35*, 900–901.
[7] S. de Feyter, P. C. M. Grim, M. Rücker, P. Vanoppen, C. Meiners, M. Sieffert, S. Valiyaveettil, K. Müllen, F. C. de Schryver, *Angew. Chem.* **1998**, *110*, 1281–1284; *Angew. Chem. Int. Ed.* **1998**, *37*, 1223–1226.
[8] D. P. E. Smith, *J. Vac. Sci. Technol. B* **1991**, *9*, 1119–1125.
[9] J. V. Selinger, Z. G. Wang, R. F. Bruinsma, C. M. Knobler, *Phys. Rev. Lett.* **1993**, *70*, 1139–1142.
[10] R. Viswanathan, J. A. Zasadzinski, D. K. Schwartz, *Nature* **1994**, *368*, 440–443.
[11] S. J. Sowerby, W. M. Heckl, G. B. Petersen, *J. Mol. Evol.* **1996**, *43*, 419–424.
[12] F. Charra, J. Cousty, *Phys. Rev. Lett.* **1998**, *80*, 1682–1685.
[13] T. A. Jung, R. R. Schlittler, J. K. Gimzewski, *Nature* **1997**, *386*, 696–698.
[14] G. P. Lopinski, D. J. Moffatt, D. D. M. Wayner, R. A. Wolkow, *Nature* **1998**, *392*, 909–911.
[15] S. de Feyter, A. Gesquière, P. C. M. Grim, F. C. de Schryver, S. Valiyaveettil, C. Meiners, M. Sieffert, K. Müllen, *Langmuir* **1999**, *15*, 2817–2822.
[16] M. Böhringer, K. Morgenstern, W. D. Schneider, M. Wühn, C. Wöll, R. Berndt, *Surf. Sci.*, in press.
[17] M. Böhringer, K. Morgenstern, W. D. Schneider, R. Berndt, F. Mauri, A. de Vita, R. Car, *Phys. Rev. Lett.* **1999**, *83*, 324–327.
[18] M. Böhringer, K. Morgenstern, W. D. Schneider, R. Berndt, *Angew. Chem.* **1999**, *111*, 832–834; *Angew. Chem. Int. Ed.* **1999**, *38*, 821–823.
[19] A. J. Fisher, P. E. Blöchl, *Phys. Rev. Lett.* **1993**, *70*, 3263–3266.
[20] a) D. Andelman, P. G. de Gennes, *C. R. Acad. Sci.* **1988**, *307*, 233; b) D. Andelman, *J. Am. Chem. Soc.* **1989**, *111*, 6536–6544.
[21] R. Gaisch, J. K. Gimzewski, B. Reihl, R. R. Schlittler, M. Tschudy, W. D. Schneider, *Ultramicroscopy* **1992**, *42–44*, 6844.

  0570-0833/00/3904-0795 $ 17.50+.50/0